Dairy cows inoculated with highly pathogenic avian influenza virus H5N1

https://doi.org/10.1038/s41586-024-08166-6

Received: 29 July 2024

Accepted: 8 October 2024

Published online: 15 October 2024

Open access



Amy L. Baker^{1™}, Bailey Arruda¹, Mitchell V. Palmer¹, Paola Boggiatto¹, Kaitlyn Sarlo Davila¹, Alexandra Buckley¹, Giovana Ciacci Zanella¹, Celeste A. Snyder¹, Tavis K. Anderson¹, Carl R. Hutter¹, Thao-Quyen Nguyen¹, Alexey Markin¹, Kristina Lantz², Erin A. Posey², Mia Kim Torchetti², Suelee Robbe-Austerman², Drew R. Magstadt³ & Patrick J. Gorden³

Highly pathogenic avian influenza (HPAI) H5N1 haemagglutinin clade 2.3.4.4b was detected in the USA in 2021. These HPAI viruses caused mortality events in poultry, wild birds and wild mammals. On 25 March 2024, HPAI H5N1 clade 2.3.4.4b was confirmed in a dairy cow in Texas in response to a multistate investigation into milk production losses¹. More than 200 positive herds were identified in 14 US states. The case description included reduced feed intake and rumen motility in lactating cows, decreased milk production and thick yellow milk^{2,3}. The diagnostic investigation revealed viral RNA in milk and alveolar epithelial degeneration and necrosis and positive immunoreactivity of glandular epithelium in mammary tissue. A single transmission event, probably from birds, was followed by limited local transmission and onward horizontal transmission of H5N1 clade 2.3.4.4b genotype B3.13 (ref. 4). Here we sought to experimentally reproduce infection with genotype B3.13 in Holstein yearling heifers and lactating cows. Heifers were inoculated by an aerosol respiratory route and cows by an intramammary route. Clinical disease was mild in heifers, but infection was confirmed by virus detection, lesions and seroconversion. Clinical disease in lactating cows included decreased rumen motility, changes to milk appearance and production losses. Infection was confirmed by high levels of viral RNA detected in milk, virus isolation, lesions in mammary tissue and seroconversion. This study provides the foundation to investigate additional routes of infection, pathogenesis, transmission and intervention strategies.

HPAI H5N1 viruses of the goose/Guangdong lineage in the haemagglutinin clade 2.3.4.4b were detected in the USA in 2021 following widespread dispersion across Asia and Europe⁵. H5N1 viruses in this clade were detected across the USA in mortality events in wild bird species and wild mammals. Additionally, outbreaks occurred in numerous commercial and backyard poultry premises, leading to culling to control the spread. On 25 March 2024, the National Veterinary Services Laboratories of the US Department of Agriculture confirmed a case of HPAI H5N1 clade 2.3.4.4b genotype B3.13 in a dairy cow in Texas in response to a multistate investigation into milk production losses. Additional outbreaks were rapidly identified in Texas as well as eight other US states. As of 12 September 2024, more than 200 cases had been confirmed in 14 states¹. The typical case description on the affected dairy farms included reduced feed intake and rumination in lactating cows, rapid drop in milk production, and affected cows with thick yellow milk with flecks and/or clots^{2,3}. The diagnostic investigation revealed low cycle threshold (Ct; high viral load) detections of viral RNA by quantitative real-time PCR with reverse transcription (RT-qPCR) in milk, mammary tissue with alveolar epithelial degeneration and necrosis with intraluminal sloughing of cellular debris, and positive immunoreactivity of glandular epithelium with nuclear and cytoplasmic labelling by immunohistochemistry (IHC). Deceased domestic cats located on affected dairy farms that presented with neurologic and respiratory signs were also confirmed to be infected with the same H5N1 clade 2.3.4.4b B3.13 genotype, as were several peridomestic wild birds found around or near affected premises.

A genomic and epidemiologic investigation demonstrated that a single transmission event from a vian species preceded the multistate cattle outbreak⁴. The movement of preclinical or subclinical lactating dairy cows was the main contributor to spread among the US dairy premises. Sequence analysis thus far revealed highly similar genomes among cattle detections with little evolution or known mammalian adaptation markers⁴. Several human infections were reported with H5N1 clade 2.3.4.4b, and although some were severe or fatal, the human detections thus far associated with the dairy outbreak in the USA were mild⁶⁻⁸. However, transmission in multiple host species, particularly mammals, raises the concern for mammalian adaptation that may lead to increased potential for human infection and/or transmission.

Although a few sporadic detections of human seasonal influenza A virus (IAV) or antibodies were previously reported in experimental

Virus and Prion Research Unit, National Animal Disease Center, Agricultural Research Service, United States Department of Agriculture, Ames, IA, USA. 2National Veterinary Services Laboratories, Animal and Plant Health Inspection Service, United States Department of Agriculture, Ames, IA, USA. 3 Veterinary Diagnostic and Production Animal Medicine, Iowa State University, Ames, IA, USA. [™]e-mail: amv.l.baker@usda.gov

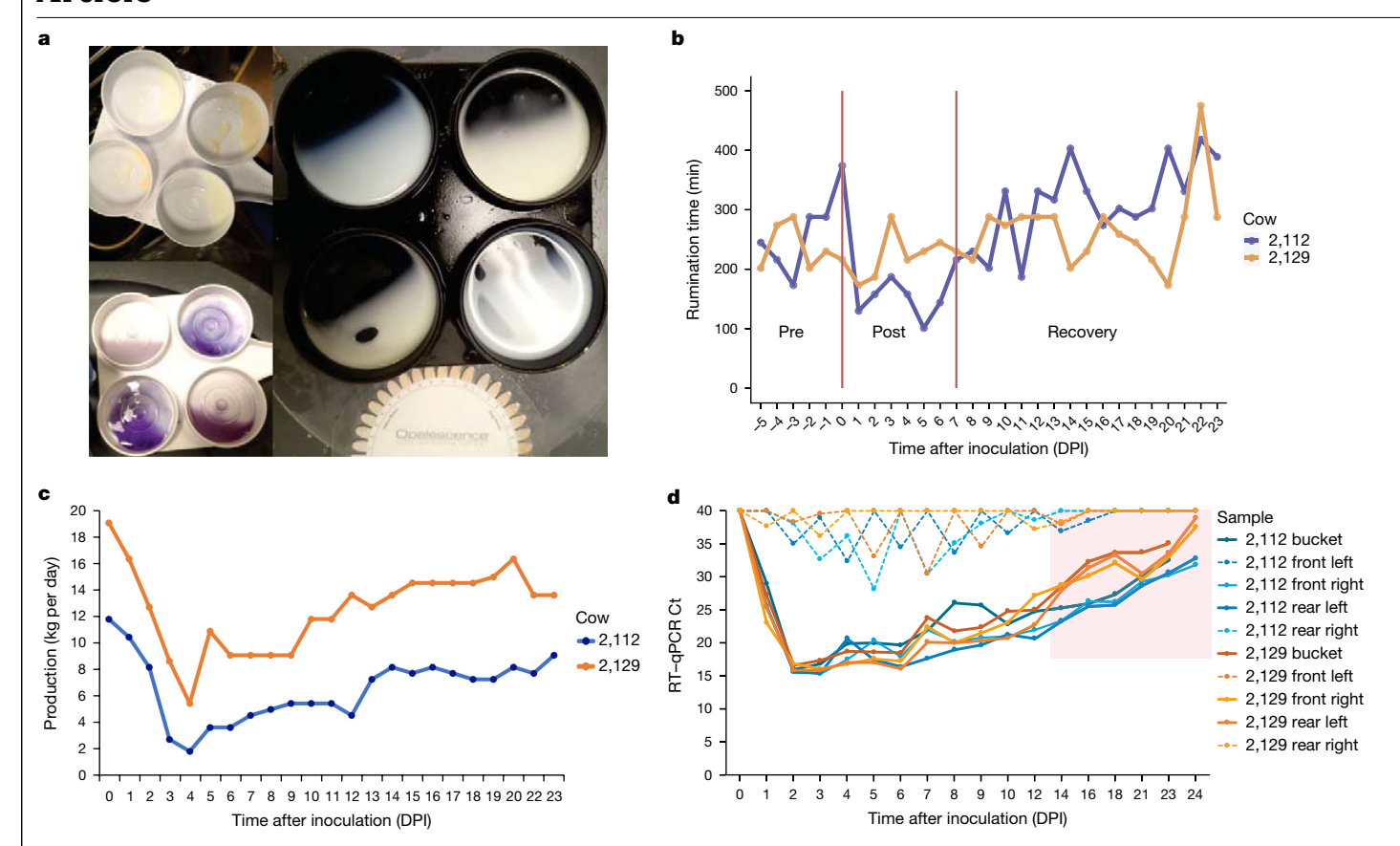


Fig. 1 | Clinical signs and viral detection in lactating dairy cows.

a, Representative milk sampling demonstrating thickening, flakes or clots, and change in colour in the upper left and right photographs, and gel formation in positive California mastitis tests in the lower left photograph. In all photos, changes were observed in the inoculated front right and rear left quarters in the upper right and lower left cups of the milk collection paddle in each photo. **b**, Daily rumination time in minutes for cow 2,112 (blue) and cow 2,129 (orange) measured using an ear-tag accelerometer sensor. Rumination time decreased at 1 DPI and recovered to pre-challenged levels at 7 DPI. c, Each individual milking machine bucket was weighed once daily to monitor production, for cow 2,112 (blue) and cow 2,129 (orange). Milk production steadily declined from 1 to 4 DPI, remained low until 10-12 DPI, and was 71-77% of pre-inoculation

production at 23 DPI. d, Milk was stripped from each teat before milking and a sample was taken from the bucket after milking, for cow 2,112 (blue) and cow 2,129 (orange). An RT-qPCR assay detected viral RNA beginning on 1 DPI until study termination at 24 DPI in the inoculated quarters (solid lines), with Ct on the yaxis and DPI on the xaxis. The positive detections in non-inoculated quarters (dashed lines) were probably cross-contamination due to the nonsterile collection of milk from each teat. The pink shading indicates time points when live virus isolation was attempted from the bucket samples and samples were negative by egg inoculation. One inoculated quarter from cow 2,112 was positive for virus isolation on 12 DPI, but all tested samples beyond 12 DPI were negative for virus isolation.

inoculation of dairy $cows^{9,10}$ or associated with milk production $loss^{11,12}$, the Texas cases in 2024 were the first reports of HPAI of any subtype causing viral mastitis in lactating dairy cows. At the time we initiated these experiments, the route of infection and transmission between cows was unknown. Transmission between farms was linked to movement of live lactating cows, yet within-farm spread to resident cows was observed within days or weeks following movement without a clear pattern of transmission consistent on all farms. Here we sought to experimentally reproduce infection of dairy cattle with genotype B3.13 in Holstein yearling heifers through an aerosol respiratory route and in lactating cows through an intramammary route.

Phylogenetic analysis of study strain

The phylogenetic tree topology (Extended Data Fig. 1) with B3.13 genotype strains collected from dairy cattle between March and May 2024 was congruent with earlier analyses⁴. The HA gene tree indicated a single monophyletic clade; following the introduction of the B3.13 virus genotype into dairy cattle in late 2023 (ref. 4), it persisted and rapidly spread through cattle populations. There was no evidence of reassortment, and all viruses detected in dairy cattle were classified as B3.13 genotype maintaining the new polymerase basic 2 (PB2) and nucleoprotein (NP) gene that had been acquired in migratory birds before the spillover⁴. The HA gene tree and the phylogenomic tree had little evidence for directional selection with long external branches relative to internal branches, and many viruses that were identical. These data suggested a founder effect in which a single genotype was introduced into a new population of susceptible hosts¹³. The TX/24 challenge strain was 99.94% identical to a B3.13 whole-genome consensus strain (nine nucleotide substitutions across the genome); the TX/24 HA gene had only two synonymous substitutions and the protein was identical to a consensus B3.13 HA amino acid sequence.

Clinical observations

Following transition to containment, rumen motility, feed consumption and milk production stabilized in the lactating cows by the time of inoculation. Following inoculation, both cows showed signs of mastitis with a positive California mastitis test and milk colour and consistency changes beginning at 2 days post inoculation (DPI) and lasting until approximately 14 DPI, only in the inoculated quarters (Fig. 1a). The peak average colour change score in the milk from inoculated quarters

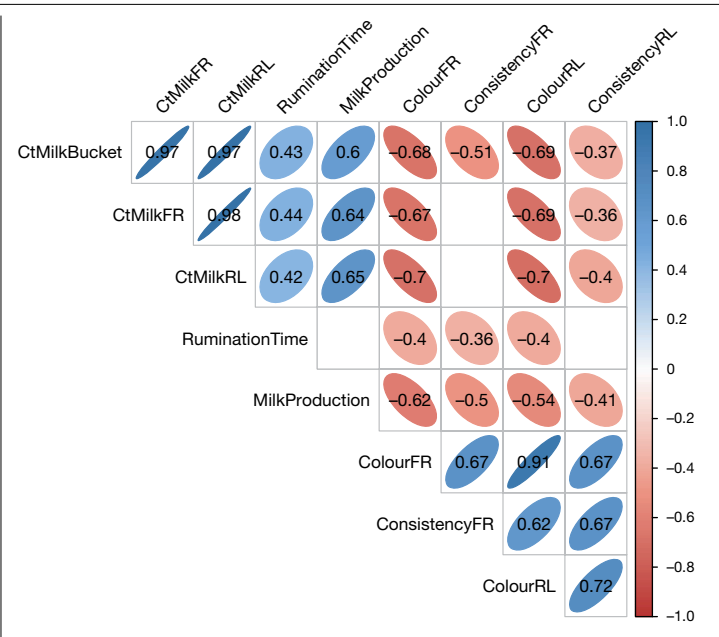


Fig. 2 | Correlation between viral RNA detection and clinical signs. Significant (P < 0.05, two-sided) Pearson correlation coefficients between Ct values for milk samples from the bucket (n = 34) as well as the inoculated teats (front right (FR) (n = 34) and rear left (RL) (n = 34)) and rumination time (n = 46), milk production (n = 44) and consistency (n = 48) and colour (n = 48) scores of milk from the inoculated teats across all time points. Empty squares in the matrix indicate the correlation was not significant (P < 0.05, two-sided).

from both cows was 6.5 on a yellow to brown scale (0-12) on 5 and 6 DPI. The milk was yellow, thicker and contained flakes and clots of debris from affected quarters during the same time period. Rumen motility markedly declined on 1 DPI and began recovering after 7 DPI (Fig. 1b). Milk production steadily declined from 1 to 4 DPI, remained low until 10–12 DPI, and was 71–77% of pre-inoculation production (0 DPI) at 23 DPI (Fig. 1c). The cows showed signs of lethargy, reduced feed intake, self-resolving watery diarrhoea or dry faeces, and intermittent clear nasal discharge throughout the 24-day observation period. Neurologic signs were not observed.

The heifer calves exhibited no overt signs of illness, with only transient increases in nasal secretions observed. Other clinical parameters indicative of illness were not consistently observed in the lactating cows or heifer calves.

Virus detection

Milk stripped from inoculated mammary quarters and the post-milking bucket sample were continuously positive by RT-qPCR from 1 DPI until the end of the study (Fig. 1d). Although stripped milk from noninoculated quarters had a Ct below 35, the detection was not consistent over consecutive days and never progressed to low Ct values indicative of live virus replication in those mammary glands. Milk bucket samples subjected to virus isolation were positive on 5, 7 and 10 DPI and negative on 12, 14, 16 and 18 DPI. One inoculated quarter from cow 2,112 was positive for virus isolation on 12 DPI, but all tested mammary quarter samples beyond 12 DPI were negative for virus isolation.

There were strong positive correlation coefficients between Ct values from the milk bucket and infected quarters with rumination and milk production. As Ct decreased (higher viral load) so did rumination and milk production. There were also strong negative correlation coefficients between milk Ct values and colour and consistency scoring, as Ct decreased (higher viral load), colour and consistency scores increased (Fig. 2). Only one nasal swab (Ct 33.1) from cow 2,112 and one ocular swab (Ct 34.7) from cow 2,129 on 3 DPI had RT-qPCR Ct \leq 35; all remaining clinical samples had RT-qPCR Ct greater than 35 cycles or undetected. No faecal swab or blood samples were positive by RT-qPCR at any time point. From the broad range of samples collected at necropsy, mammary tissue from inoculated quarters and supramammary lymph nodes had RT- α PCR Ct \leq 35, and an inguinal lymph node and one inoculated mammary tissue had a Ct of between 35 and 38. All other samples were not within RT-qPCR detection limits. (Extended Data Table 1).

Nasal, or opharyngeal, saliva and ocular samples collected from the aerosol-inoculated heifers sporadically had RT-qPCR Ct ≤ 35 (Extended Data Table 2). Heifer 2,316 had nasal swabs with Ct ≤ 35 from 1 to 5 DPI and at 7 DPI. Viral RNA was also detected across multiple days in oropharyngeal swabs, ocular swabs or saliva from heifer 2,316. Viable virus isolation was attempted on clinical samples with $Ct \le 35$, and 2-5- and 7-DPI nasal swabs from heifer 2.316 were virus isolation positive. This heifer was euthanized for necropsy on 7 DPI, so no further ante-mortem samples were collected. Each of the other three heifers tested positive by RT-qPCR on at least one time point between 1 and 7 DPI, but sporadically and not on consecutive days. Heifer 2,311 had one FLOQ or ophary ngeal swab that was positive for virus isolation on 3 DPI. No faecal swab or blood samples were positive by RT-qPCR at any time point. The sham-inoculated negative control heifer 2,309 had no RT-qPCR detections as expected. From the broad range of samples collected at the 7-DPI necropsy, lung tissue from both heifers (accessory lobes and cranial part of the left cranial lobe) had RT-qPCR $Ct \le 35$, and a retropharyngeal lymph node, a lung lobe (caudal part of the right cranial lobe and middle lobe) and a turbinate sample had a Ct between 35 and 38. All other samples at DPI 7 as well as all samples from the 20-DPI necropsy were not within RT-qPCR detection limits (Extended Data Table 2).

Single nucleotide variant analysis of samples

Across 82 clinical samples collected from the experimentally inoculated cattle, we identified within-host single nucleotide variants that were present at low frequencies (present in greater than 0.5%) across the genome. We matched a custom database of variants of interest that could potentially provide a selective advantage and alter virus phenotype. Overall, there were 3,960 single nucleotide variants present at low frequencies, of which 2,676 altered the amino acid with nonsynonymous changes (Extended Data Table 3). Of the amino-acid changes detected, only 12 had previously been associated with known functional changes. We detected low-frequency variants associated with changes in pathogenicity or virulence in the gene segments encoding matrix (T139A), non-structural (T91N, T91A, D92E, D92N, T94A, L95P, S99P, D101N, D101G and D125N) and PB1 (R622Q) proteins. We also detected low-frequency variants associated with mammal adaptation in non-structural (F103S) and PB2 (L631P) proteins. Despite these low-frequency detections, none had allele frequencies greater than 11%; however, if any such mutations provided a selective advantage, this phenotype could be selected for increased frequency in the population. There was a marginal trend for more variants and increased nonsynonymous sites on DPI 1-3 and 9-14; however, this was not significant as the sample sizes were small, and the differences had overlapping ranges (Extended Data Table 3).

Antibody responses

The dairy cows inoculated by the intramammary route were negative for NP antibody in serum before inoculation, became positive on 7 DPI using a sample/negative ratio cutoff of 0.6, and remained positive on all subsequent sample time points (Extended Data Table 4a). Fresh stripped milk from both cows was also positive by NP enzyme-linked immunosorbent assay (ELISA) by 9 DPI. Both cows were seropositive by haemagglutinin inhibition (HI) assay on 24 DPI and by virus neutralization antibody assay on 14 and 24 DPI (Extended Data Table 4b).

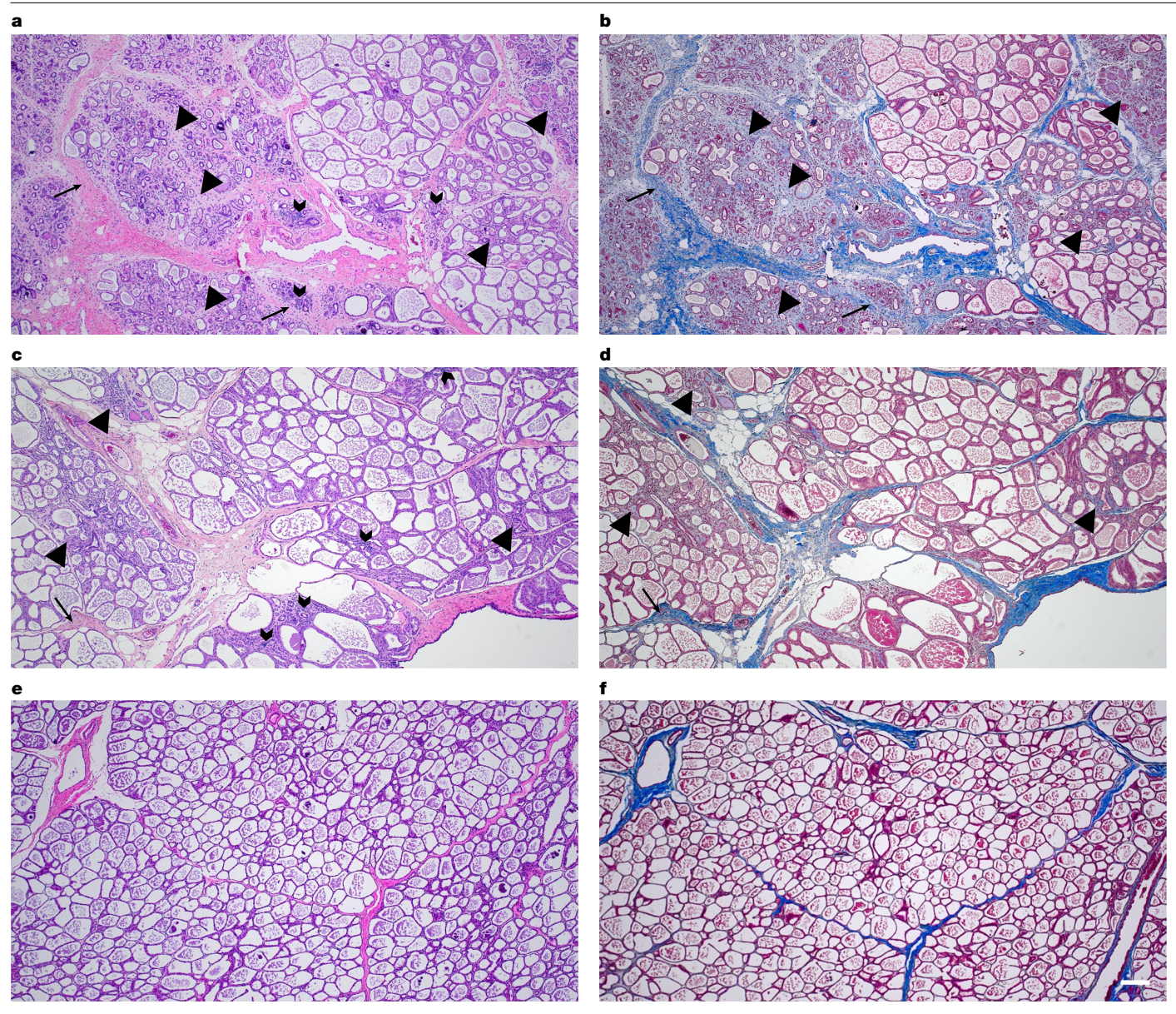


Fig. 3 | **Fibrosis in inoculated mammary gland tissue. a, c**, Representative photomicrographs of the interlobular (arrowheads) and intralobular (arrows) fibrosis and inflammatory infiltrate (chevrons) of the left rear mammary gland in cows 2,112 (a) and 2,129 (c). **b, d**, A matched Masson's trichrome stain (fibrosis is blue) demonstrates the extent of fibrosis in cows 2,112 (b) and 2,129 (d).

e,f,A representative photomicrograph showing haematoxylin–eosin (e) and Masson's trichrome (f) staining in a non-inoculated teat (left front) of cow 2,112 for comparison. All photomicrographs are at ×100 magnification and the scale bar (200 μm) applies to all panels.

Milk samples collected from each quarter on 24 DPI were tested by HI with reciprocal titres of 10–40, with both cows having quarters above and below the HI positive cutoff of \geq 40. However, virus neutralization antibody assays in inoculated quarters were positive on 9 DPI for cow 2,129 and on 12 DPI for cow 2,112. The uninoculated quarters from both cows remained below the positive cutoff titre of 1:40. Two of the heifer calves were positive for NP antibodies on 7 DPI, and the remaining two seroconverted between 9 and 13 DPI (Extended Data Table 4c). One calf was positive by HI assay and the calf with a later NP antibody response was suspect by HI assay at 20 DPI. The sham-inoculated negative control remained seronegative as expected.

Pathologic evaluation

Minimal multifocal obstructive atelectasis was present in heifer 2,316 (Extended Data Fig. 2). In the lactating cows, lesions considered

incidental were observed and included a unilateral locally extensive pleural adhesion and transparent, straw-coloured abdominal fluid in cow 2,112 and interlobular pulmonary oedema in cow 2,129. Macroscopic evaluation of the remaining tissues was unremarkable.

Similar histologic lesions were present in the left rear mammary gland (inoculated) of both dairy cattle. Fibrous connective tissue replaced 15% to 50% of secretory alveoli and ducts, both intralobular and interlobular, of multifocal lobules (Fig. 3a–d). The remaining secretory alveoli in affected lobules were commonly shrunken and lined by small, attenuated or swollen, vacuolated epithelial cells (atrophy and degeneration). Both interlobular and intralobular fibrous connective tissue contained multifocal aggregates of segmental to circumferential perialveolar or periductular mononuclear inflammatory cells predominated by lymphocytes and plasma cells. The remaining secretory alveoli and ducts contained secretory product admixed with occasional foamy cells (macrophages or foam cells) or

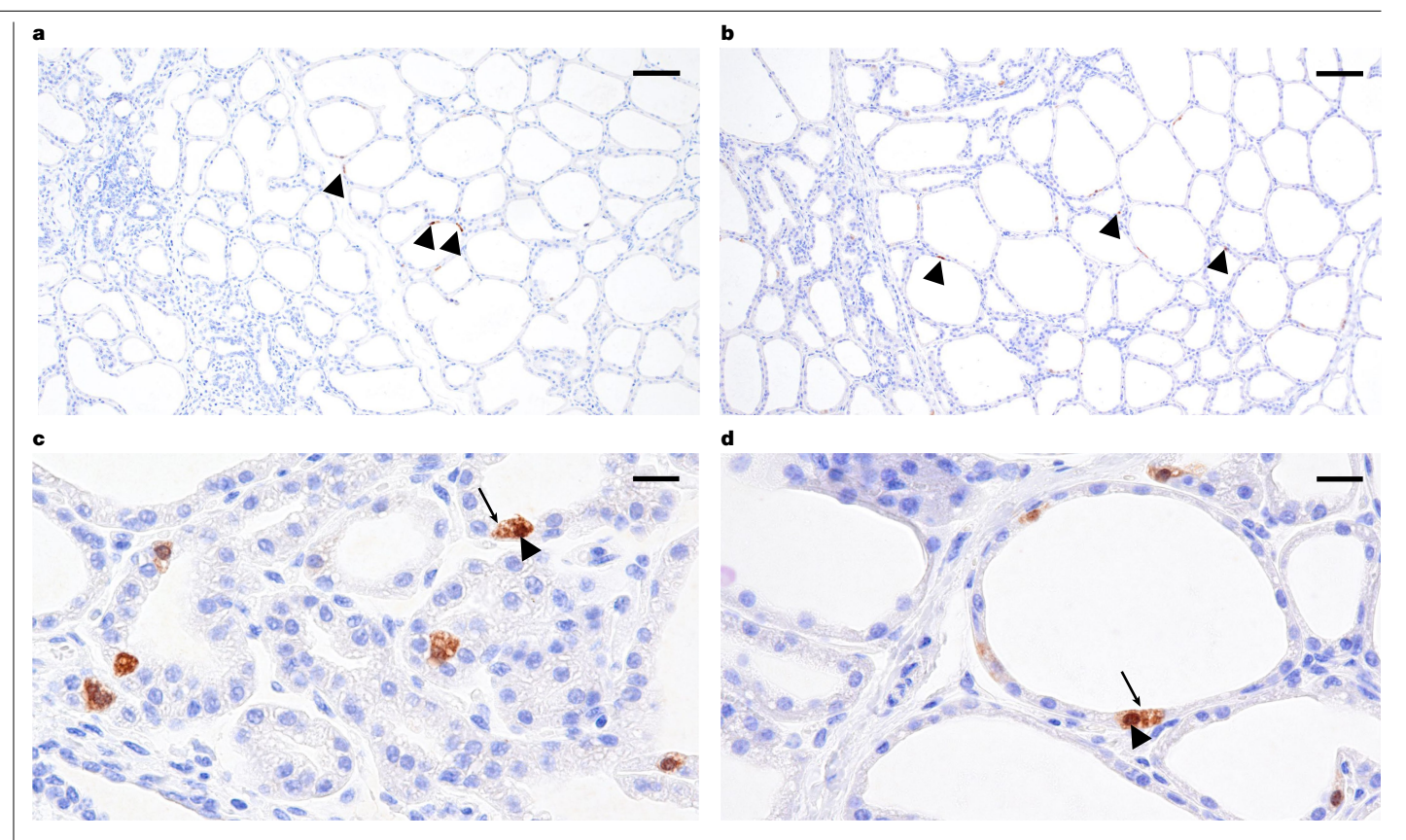


Fig. 4 | IHC in mammary tissue. a-d, IHC detection of IAV antigen in epithelial cells lining secretory alveoli of the left rear mammary glands (arrowheads in a,b) with higher-magnification images showing staining in the cytoplasm

(arrows in c,d) and nucleus (arrowheads in c,d), for cows 2,112 (a,c) and 2,129 (**b**,**d**). Photomicrographs at ×100 (**a**,**b**) and ×400 (**c**,**d**) magnification. Scale bars, $100 \, \mu m \, (\mathbf{a}, \mathbf{b}) \, \text{and} \, 20 \, \mu m \, (\mathbf{c}, \mathbf{d})$.

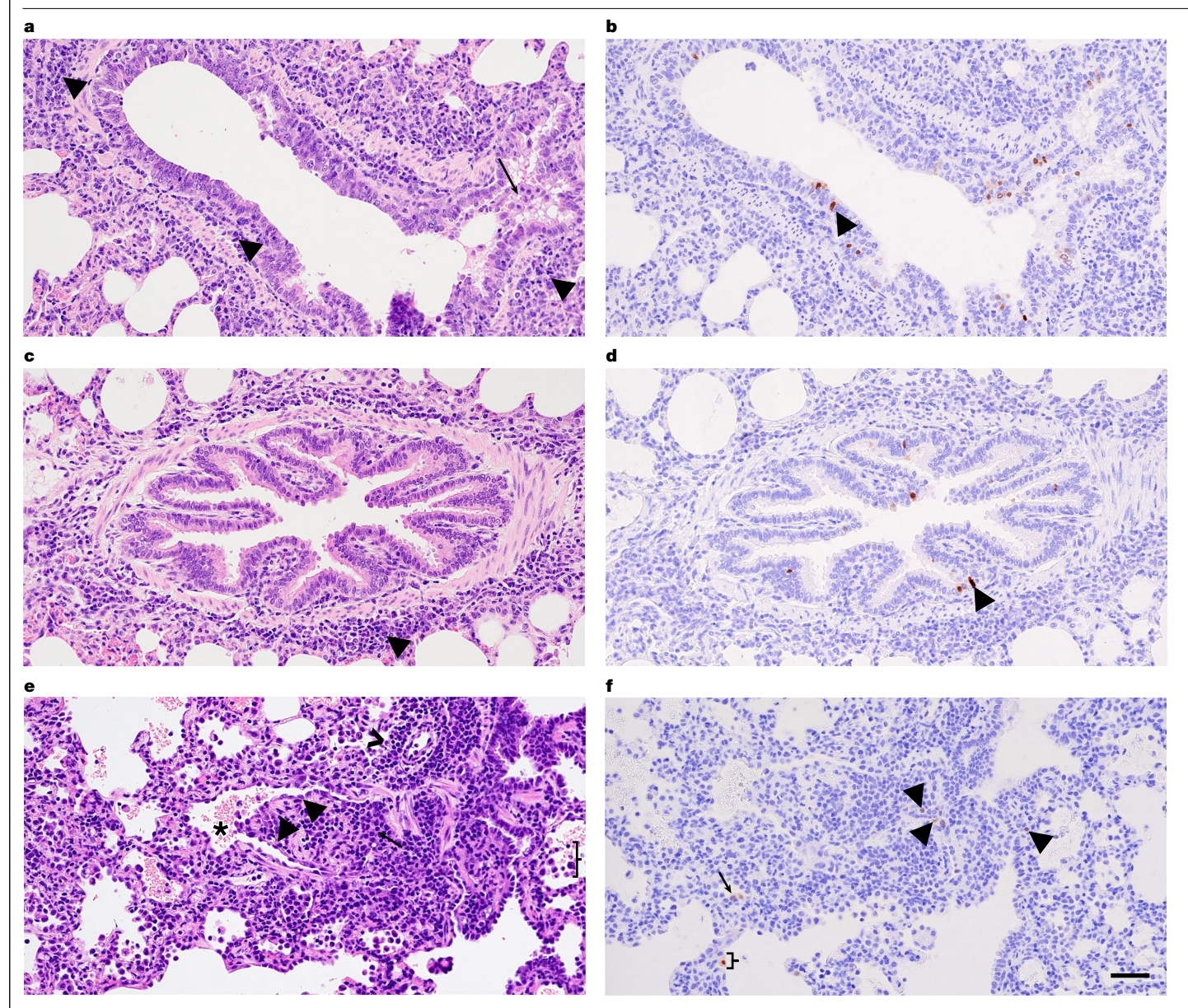
rarely deeply basophilic, concentrically lamellated foci (corpora amylacea). Non-affected to minimally affected glandular tissue commonly contained moderately to well-developed secretory alveoli. Histologic evaluation of the non-inoculated mammary quarters (left front and right rear) was characterized by well-developed secretory epithelium that contained fluid and no to minimal intralobular or interlobular fibrosis and no to rare aggregates of mononuclear leukocytes predominated by lymphocytes and plasma cells (Fig. 3e,f). A summary of microscopic findings including IHC is presented in the data file in Zenodo (see Data availability section).

IAV NP antigen was detected in the cytoplasm and nucleus of epithelial cells lining secretory alveoli in the inoculated mammary gland quarters of both cows at 24 DPI (Fig. 4a-d). IAV NP antigen was also detected in the light zone of multiple germinal centres of the supramammary lymph node of cow 2,129 (Extended Data Fig. 3).

In the heifers necropsied at 7 DPI, minimal lesions consistent with IAV infection were focused on conducting airways. The interstitium of a bronchiole of the caudal part of the left cranial lung lobe of heifer 2,311 was minimally circumferentially expanded by a predominance of lymphocytes and plasma cells. IAV was detected by IHC within the respiratory epithelial cells lining this conducting airway (Fig. 5a-d). Bronchiolitis obliterans was present in the caudal part of the left cranial lung lobe of heifer 2,316 (Fig. 5e). The lumen of a focal bronchiole was 80% occluded by a polyp of fibrocytes and fibrin admixed with inflammatory cells and lined by markedly attenuated epithelium. The surrounding interstitium was mildly circumferentially expanded by lymphocytes and plasma cells. Scant IAV NP antigen was detected in the remaining epithelial cells of the affected bronchiole, adjacent type II pneumocytes and probable alveolar macrophage (Fig. 5f). Additional histologic lesions were observed in both cows and heifers; however, the role of IAV infection in the development of these lesions could not be defined by IHC or lesion character was not consistent with the disease time course.

Discussion

We describe two successful models of experimental infection in cattle with an H5N1 clade 2.3.4.4b genotype B3.13 strain. Signs of clinical disease from a respiratory route of exposure were variable and may not be recognized under field conditions. Experimentally inoculated cows showed clinical signs for 7-14 days, with changes to the milk similar to those documented in field reports, including change in colour from white to yellow, thickening and presence of flakes or clots^{2,14}. From 14 to 24 DPI, after cows appeared to be recovering, viral RNA was still detected in the milk and replicating virus was present in the inoculated mammary gland quarters as detected by IHC on 24 DPI. However, viable virus was not found in the pooled milking machine bucket or individual quarter milk samples after 12 DPI. The detection of virus neutralization antibodies in the inoculated quarters coincided with negative virus isolation. Additional functional antibody studies are needed for use with milk as the sample type to understand when neutralizing antibodies appear and how long they last in larger numbers of animals. All calves and cows seroconverted during the study, confirming infection from both routes of inoculation. The commercial ELISA used to detect NP antibodies had not been validated by the manufacturer for bovine serum or milk at the time of this study. The kit cutoff value is 0.5 for avian species and included validation for H5N1 strains. The kit cutoff value is 0.6 for pigs, but based on H1 and H3 subtypes. Robust validation with known positive and known negative bovine samples is needed for establishing a sensitive and specific cutoff for this host



 $\label{eq:Fig.5} \textbf{Histopathologic changes in heifer lung tissue. a}, \textit{Peribronchiolar mononuclear cell inflammatory infiltrate (arrowheads) and accumulation of intraluminal inflammatory cells (arrow) in a bronchiole in the cranial part of the left cranial lung lobe of heifer 2,311.$ **b**, Replication of HPAI virus in the respiratory epithelium lining the affected bronchiole of heifer 2,311 shown in**a**, as demonstrated by IHC (arrowheads).**c**, Peribronchiolar mononuclear cell inflammatory infiltrate (arrowheads) in another bronchiole in the cranial part of the left cranial lung lobe of heifer 2,311.**d**, Replication of HPAI virus in the respiratory epithelium lining the affected bronchiole of heifer 2,311 shown in**c**, as demonstrated by IHC (arrowheads).**e**, Bronchiolitis obliterans in heifer 2,316. The lumen of a bronchiole (asterisk) is partially occluded by a polyp

lined by attenuated epithelial cells (arrowheads). The polyp is composed of fibroblasts, fibrin and lymphocytes (arrow). Adjacent alveoli contain increased inflammatory cells (probable alveolar macrophages; brace). An adjacent arteriole is circumferentially surrounded by a mononuclear cell inflammatory infiltrate composed predominately of lymphocytes and fewer plasma cells (chevron). **f**, Replication of HPAI virus in the respiratory epithelium lining the affected bronchiole of heifer 2,316 as demonstrated by IHC (arrowheads), and in probable type II pneumocytes (arrow) and alveolar macrophage (brace). All photomicrographs are at $\times 200$ magnification and the scale bar (50 μ m) applies to all panels.

and subtype and has now been reported¹⁵, and owing to the known exposure, consecutive sampling and steady decline of the sample/ negative optical density ratios, we used ≤0.6 as the cutoff for positivity.

The amount and duration of virus shed in milk from the inoculated mammary quarters are major findings of this study and point to the mammary gland and milk as primary sources of virus spread within and between dairy herds. This is consistent with the finding that movement of lactating cows was a primary epidemiologic link between the earliest herds involved in the outbreak 4 . Virus replication in infected mammary glands was considerably more than that expected from lungs of animals infected with host-adapted IAV 16 . This is probably, at

least in part, due to the cellular structure and physiology of the lung compared to those of the mammary gland. Although IAV-susceptible epithelial cells line the conducting airways, these airways make up a minority of the lung structure. On the basis of both NP IHC from naturally infected dairy cattle and lectin staining, most of the mammary gland is composed of IAV-susceptible epithelial cells^{2,17}. Moreover, there is regular sloughing of epithelial cells and secretion of milk fat globules. Following release from the secretory epithelial cell, milk fat globules are bordered by epithelial cell membrane. Milk fat globules can also have a membrane crescent that consists of epithelial cell cytoplasm. Both the epithelial cell membrane and the crescent of milk fat

globules may be lined by or contain non-infectious and/or infectious viral particles; however, further exploration of mammary tissue by electron microscopy is needed to confirm the role that milk fat globules play in the shedding of HPAI. The fibrosis and loss of secretory alveoli in the evaluated sections of the left rear mammary gland varied from mild to severe and were more extensive in sections evaluated in cow 2,112. A loss of secretory alveoli was also noted in directly IAV-inoculated mammary glands of nursing ferrets and mothers of IAV-infected infant ferrets¹⁸. The extent to which secretory alveoli were lost and replaced by fibrous connective tissue within the affected quarter or quarters may account for the variable return to milk production of individual animals following HPAI infection reported by farms². The long-term impact of mammary fibrosis in recovered cows in subsequent lactation cycles remains to be determined. Fibrosis is not a common finding in the lung following uncomplicated IAV infection and supports a divergent immunopathogenesis^{18,19}. This may be due to the need for limiting inflammatory responses in an organ that is vital to life, the number of cells susceptible to infection, and mechanisms of host viral clearance through immune responses. This hypothesis is further supported by the systemic clinical signs observed in the dairy cattle that included depression, anorexia and drop in rumen motility. The presence of replicating virus in the inoculated mammary quarters at the time of necropsy at 24 DPI suggests a longer course for this organ to effectively clear the virus in comparison to that of the organs of the respiratory tract in which virus becomes undetectable around 7 DPI (ref. 19). Although fibrosis would probably result in decreased milk production for animals in the field, prevention of fibrosis could be a primary variable for vaccine efficacy trials, along with significant reduction in virus titres. The application of a trichrome strain effectively demonstrated the amount of fibrous connective tissue present within glands, and sections could be taken after the duration and quantity of viral shedding were characterized.

No to mild respiratory signs have been reported in many affected dairy herds in the USA14 and relatively few bovine respiratory diagnostic samples have been confirmed to be positive for H5N1 HPAI. The clinical signs, RT-qPCR results, macroscopic lesions, histologic findings and antigen distribution of this study align with these field observations. However, the mild macroscopic and histologic lung lesions, detection of replicating IAV by IHC in the lower respiratory tract, and RT-qPCR detection with virus isolation in two upper respiratory swabs confirmed a respiratory phase of infection following aerosol inoculation, similar to a previous study that experimentally inoculated calves with a different genotype of H5N1 (ref. 20). Although respiratory infection was limited in the four heifers, the detection of viable virus in two out of four implies that there is a role for the respiratory route as a mode of infection and transmission that may be important in an animal facility that commonly holds hundreds of animals. If natural exposure to respiratory secretions or infected milk leads to production of neutralizing antibodies, it may prove beneficial in preventing mastitis if the cow is subsequently re-exposed by the intramammary route during the milking process.

The enteric signs that included both diarrhoea (cow 2,129) and dry faecal material (cow 2,112) noted in this study also align with reports from the field and justify the initial clinical differential diagnosis of an atypical enteric bovine coronavirus infection for the milk drop syndrome. Minimal lesions were observed in the jejunum of both cows and cannot be definitively attributed to HPAI H5N1 infection. The loss of crypts and expansion of the lamina propria by fibrous connective tissue is a chronic change present at 24 DPI, and owing to study timing, tissues were collected days after enteric signs were noted. RT-qPCR did not detect HPAI in any rectal swab at any time point or in the jejunum or faeces of inoculated animals at necropsy, but low levels of replication in the upper gastrointestinal system cannot be ruled out on the basis of the timing of the necropsy. Additional studies focused on pathologic assessment and antigen distribution at multiple time points following

inoculation should be conducted to more thoroughly evaluate tissue tropism at the cellular level.

The interspecies transmission of H5N1 clade 2.3.4.4b to many mammal species, now including cattle with genotype B3.13, is unprecedented in our understanding of avian-adapted IAV^{21,22}. This raises concern for other mammalian hosts, including pigs and other livestock and pets, and particularly for humans. The human cases in the USA have been clinically mild and limited in number^{6,7}, but concern remains as H5N1 continues to expand into new hosts, spread geographically and reassort with other avian or mammalian subtypes. The possibility of H5N1 becoming endemic in cattle increases as the number of infected herds continues to rise¹. Pasteurization was shown to inactivate virus, and retail milk remains negative for infectious virus, and thus is not a risk for human consumption when processed according to Food and Drug Administration standards^{23,24}. Unpasteurized milk and dairy products are a risk to humans and other animals. Milk from H5N1-positive dairy herds or from suspect cows that is diverted from the human food supply should not be fed to other farm animals and it should not be dumped without inactivation owing to the risk to surrounding farms or peridomestic wild animals.

The sustained transmission among dairy cattle is an animal health crisis owing to production and economic losses and is a public health challenge owing to occupational exposure on dairy farms and human pandemic potential. The development of reproducible experimental challenge models such as the ones described here is the essential first step to inform subsequent research on intervention and vaccination strategies. Although our study was limited in the number of animals owing to their size and high containment space requirements, we reproduced the clinical observations from the field of viral mastitis due to HPAI H5N1 infection alone and confirmed respiratory involvement. Further studies to understand transmission, refine the pathogenesis model and define the kinetics of protective immunity in cattle infected with HPAI are urgently needed.

Online content

Any methods, additional references, Nature Portfolio reporting summaries, source data, extended data, supplementary information, acknowledgements, peer review information; details of author contributions and competing interests; and statements of data and code availability are available at https://doi.org/10.1038/s41586-024-08166-6.

- Detections of Highly Pathogenic Avian Influenza (HPAI) in Livestock (USDA-APHIS, 2024); https://www.aphis.usda.gov/livestock-poultry-disease/avian/avian-influenza/hpaidetections/livestock
- Burrough, E. R. et al. Highly pathogenic avian influenza A(H5N1) clade 2.3.4.4b virus infection in domestic dairy cattle and cats, United States, 2024. Emerg. Infect. Dis. https://doi.org/10.3201/eid3007.240508 (2024).
- Caserta, L. C. et al. Spillover of highly pathogenic avian influenza H5N1 virus to dairy cattle. Nature https://doi.org/10.1038/s41586-024-07849-4 (2024).
- Nguyen, T.-Q. et al. Emergence and interstate spread of highly pathogenic avian influenza A(H5N1) in dairy cattle. Preprint at bioRxiv https://doi.org/10.1101/2024.05.01.591751 (2024).
- Bevins, S. N. et al. Intercontinental movement of highly pathogenic avian influenza A(H5N1) clade 2.3.4.4 virus to the United States, 2021. Emerg. Infect. Dis. 28, 1006-1011 (2022).
- Garg, S. et al. Outbreak of highly pathogenic avian influenza A(H5N1) viruses in U.S. dairy cattle and detection of two human cases - United States, 2024. MMWR Morb. Mortal. Wkly Rep. 73 501-505 (2024)
- Uyeki, T. M. et al. Highly pathogenic avian influenza A(H5N1) virus infection in a dairy farm worker, N. Engl. J. Med. 390, 2028-2029 (2024).
- CDC reports fourth human case of H5 bird flu tied to dairy cow outbreak. CDC Newsroom https://www.cdc.gov/media/releases/2024/p-0703-4th-human-case-h5.html (2024).
- Mitchell, C. A., Walker, R. V. & Bannister, G. L. Preliminary experiments relating to the propagation of viruses in the bovine mammary gland. Can. J. Comp. Med. Vet. Sci. 17
- Mitchell, C. A., Walker, R. V. & Bannister, G. L. Persistence of neutralizing antibody in milk and blood of cows and goats following the instillation of virus into the mammary gland. Can. J. Comp. Med. Vet. Sci. 18, 426-430 (1954).
- Brown, I. H., Crawshaw, T. R., Harris, P. A. & Alexander, D. J. Detection of antibodies to influenza A virus in cattle in association with respiratory disease and reduced milk yield. Vet. Rec. 143, 637-638 (1998).

- Crawshaw, T. R., Brown, I. H., Essen, S. C. & Young, S. C. Significant rising antibody titres to influenza A are associated with an acute reduction in milk yield in cattle. Vet. J. 178, 98-102 (2008)
- 13. Peter, B. M. & Slatkin, M. The effective founder effect in a spatially expanding population. Evolution 69, 721-734 (2015).
- Highly Pathogenic Avian Influenza H5N1 Genotype B3.13 in Dairy Cattle: National Epidemiologic Brief (USDA-APHIS, 2024); https://www.aphis.usda.gov/sites/default/files/ hpai-dairy-national-epi-brief.pdf.
- Giménez-Lirola, L. G. et al. Detection and monitoring of highly pathogenic influenza A virus 2.3.4.4b outbreak in dairy cattle in the United States. Viruses 16, 1376 (2024).
- Arruda, B. et al. Divergent pathogenesis and transmission of highly pathogenic avian influenza A(H5N1) in swine. Emerg. Infect. Dis. 30, 738-751 (2024).
- 17. Nelli, R. K. et al. Sialic acid receptor specificity in mammary gland of dairy cattle infected with highly pathogenic avian influenza A(H5N1) virus. Emerg. Infect. Dis. https://doi.org/ 10.3201/eid3007.240689 (2024).
- Paquette, S. G. et al. Influenza transmission in the mother-infant dyad leads to severe disease, mammary gland infection, and pathogenesis by regulating host responses. PLoS Pathog. 11, e1005173 (2015).
- Van Reeth, K. & Vincent, A. L. in Diseases of Swine (eds Zimmerman, J. J. et al.) 576-593 (Wiley-Blackwell, 2019).
- Kalthoff, D., Hoffmann, B., Harder, T., Durban, M. & Beer, M. Experimental infection of cattle with highly pathogenic avian influenza virus (H5N1). Emerg. Infect. Dis. 14, 1132-1134
- Elsmo, E. J. et al. Highly pathogenic avian influenza A(H5N1) virus clade 2.3.4.4b infections in wild terrestrial mammals, United States, 2022. Emerg. Infect. Dis. 29, 2451-2460 (2023).

- Youk, S. et al. H5N1 highly pathogenic avian influenza clade 2.3.4.4b in wild and domestic birds: introductions into the United States and reassortments, December 2021-April 2022. Virology 587, 109860 (2023).
- 23. Updates on highly pathogenic avian influenza (HPAI). FDA https://www.fda.gov/food/ alerts-advisories-safety-information/updates-highly-pathogenic-avian-influenza-hpai (2024).
- Spackman, E. et al. Inactivation of highly pathogenic avian influenza virus with high temperature short time continuous flow pasteurization and virus detection in bulk milk tanks. J. Food. Prot. https://doi.org/10.1016/j.jfp.2024.100349 (2024).

Publisher's note Springer Nature remains neutral with regard to jurisdictional claims in published maps and institutional affiliations.



Open Access This article is licensed under a Creative Commons Attribution 4.0 International License, which permits use, sharing, adaptation, distribution and reproduction in any medium or format, as long as you give appropriate

credit to the original author(s) and the source, provide a link to the Creative Commons licence. and indicate if changes were made. The images or other third party material in this article are included in the article's Creative Commons licence, unless indicated otherwise in a credit line to the material. If material is not included in the article's Creative Commons licence and your intended use is not permitted by statutory regulation or exceeds the permitted use, you will need to obtain permission directly from the copyright holder. To view a copy of this licence, visit http://creativecommons.org/licenses/by/4.0/.

© This is a U.S. Government work and not under copyright protection in the US; foreign copyright protection may apply 2024

Methods

Strain characterization

We analysed the HPAI H5N1 genotype B3.13 virus used this study (A/dairy cattle/Texas/24-008749-002/2024: TX/24: National Center for Biotechnology Information (NCBI) PP755581-PP755588) with other B3.13 strains generated in ref. 4 and newly sequenced data collected between 16 April and 8 May 2024. IAV RNA from samples was amplified²⁵; then we generated cDNA libraries by using the Illumina DNA Sample Preparation Kit, (M) Tagmentation (Illumina) and either the iSeg or NextSeq Reagent Kit v2 (Illumina) according to the manufacturer's instructions. We performed reference-guided assembly of genome sequences using IRMA v1.1.5 (ref. 26). We aligned each gene segment using mafft v7.490 (ref. 27) and inferred maximum-likelihood phylogenetic trees for each gene segment as well as concatenated whole genomes using IQ-Tree v2.2.2 (ref. 28). These phylogenetic gene trees were used to determine how representative the TX/24 strain was relative to viruses collected between March and May 2024. This approach implemented the evaluate algorithm in PARNAS²⁹ that objectively identified the most representative strain in the B3.13 group and how near the TX/24 strain was relative to that representative strain.

Biosafety risk mitigation

Work with the HPAI H5N1 strain and subsequent animal samples was conducted in secure biosafety level 3 (BSL3) laboratory space following the Biosafety in Microbiological and Biomedical Laboratories, 6th edition³⁰, guidelines. All animal studies were carried out in a BSL3-Agriculture facility in compliance with the Institutional Animal Care and Use Committee of the National Animal Disease Center (NADC) of the US Department of Agriculture (USDA) and the Agriculture Research Service (ARS), and Federal Select Agent Program regulations.

Cow intramammary inoculation

The A/dairy cattle/Texas/24-008749-002/2024 virus was isolated from a milk sample from the outbreak investigation in 10-day-old embryonating chicken eggs²⁵ and subsequently titrated on the London line of Madin-Darby canine kidney (MDCK, International Reagent Resource) cells. Two healthy non-pregnant, lactating Holstein cows of approximately 3 years of age and 280 days in milk during their first lactation were moved from the on-site isolated NADC dairy into BSL3-Agriculture containment and acclimated for approximately 1 week before inoculation. Cows were inoculated with 1 ml of 1×10^5 tissue culture infectious dose 50 (TCID₅₀) per millilitre of the first passage of egg-grown A/dairy cattle/Texas/24-008749-002/2024 by an intramammary route in each of two quarters, front right and rear left, using a teat canula (Extended Data Fig. 4a,b). The inoculation occurred after milking and standard teat disinfection, and the teats were additionally disinfected with an alcohol wipe immediately before the procedure. After instilling, the inoculum was moved upwards into the teat sinus with gentle massage.

Calfaerosol inoculation

Five healthy Holstein heifer calves of approximately 1 year of age born in isolation on the facility were either inoculated with 2 ml of 1×10^6 TCID $_{50}$ per millilitre of A/dairy cattle/Texas/24-008749-002/2024 (n = 4) from the same virus stock as the cow inoculum or sham-inoculated with phosphate-buffered saline (PBS; n = 1) by an aerosol respiratory route. For aerosol inoculation, calves were restrained in a cattle stanchion and the inoculum was delivered by nebulization into a mask covering the nostrils and mouth (Extended Data Fig. 4c,d). A 2 ml volume of inoculum was placed into the medicine cup of the portable equine nebulizer (Flexineb E3, Nortev). Nebulization continued until all of the inoculum was delivered (approximately 3 min). Following the inoculum, 2 ml sterile PBS was nebulized through the apparatus. The portable equine nebulizer uses a vibrating mesh nebulizer, which generates aerosol droplets in the respirable range. Droplets generated

by vibrating mesh nebulizers were shown to be 3–5 μ m (ref. 31), with the manufacturer of the nebulizer reporting that 70% of the total nebulized volume resulted in droplets of <5 μ m. Aerosolized droplets that are less than 5 μ m bypass the upper respiratory tract and are deposited deep in the lower respiratory tract³².

Clinical evaluation and sample collection

In the lactating cows, rumination and other behaviours were monitored continuously using an ear-tag accelerometer sensor (CowManager SensOor, Agis Automatisering). For cows and heifers, clinical signs were visually monitored and recorded daily (Extended Data Table 5), including body temperature with a thermal microchip, respiratory effort and rate, nasal and ocular discharge, and faecal consistency. The lactating cows were milked once daily in the morning using a portable milker (Hamby). Before milking, the teats were cleaned with water, disposable paper towels, and isopropyl alcohol wipes, and milk was manually stripped from each teat into separate 50-ml tubes. The milk samples were evaluated by quarter for mastitis by the California mastitis test (ImmuCell) and for consistency and colour using a dental colour scorecard on a scale of 0-12. The remaining milk stripped by quarter was used for virus and/or antibody detection. After milking, a sample from each cow's milking machine bucket was also collected. A separate milking claw was used for each cow, and the claw, tubing and bucket were washed, degreased and disinfected (Virkon S, LanXess)

The remaining clinical samples were collected daily from cows and calves for 7 DPI and approximately every 2 days thereafter until study termination. To sample the deep pharyngeal region, a Frick cattle mouth speculum was used. Using manual restraint, the speculum was placed over the tongue to the pharynx and held there. Through the speculum, FLOQ nylon-tipped (Copan) or long cotton-tipped (SCA Health) swabs were used to collect samples of the deep oropharynx. Ocular, nasal and rectal samples were collected with FLOQ nylon swabs. Whole blood was collected through jugular venipuncture and placed into molecular transport medium (PrimeStore MTM, Longhorn) and into serum separator tubes. Saliva was collected with an absorbent pad (Super-SAL, Oasis Diagnostics).

Pathologic evaluation

All cattle were euthanized through intravenous administration of pentobarbital sodium (Fatal Plus, Vortech Pharmaceuticals). Heifers 2,311 and 2,316 and a negative control heifer were necropsied at 7 DPI, whereas the remaining two aerosol-inoculated heifers were necropsied at 20 DPI. The lactating dairy cows were necropsied at 24 DPI. At the time of necropsy, the thoracic cavity, abdominal cavity and cranium (longitudinal section) underwent macroscopic evaluation. Paired fresh and formalin-fixed tissues for RT-qPCR and microscopic evaluation, respectively, were collected (Extended Data Table 1). Formalin-fixed tissues were processed routinely for microscopic evaluation. Additional fresh samples included aqueous and vitreous humour, urine, faeces and rumen contents.

IHC targeting the NP antigen (1:2,000, GeneTex, GTX125989) of IAV was performed as previously described with the inclusion of positive (lung from an IAV-inoculated pig) and negative tissue (respiratory tissues from the control heifer and lung from a non-IAV-inoculated pig) controls¹⁶. Nasal turbinate, trachea, lung, tracheobronchial lymph node, supramammary lymph node (lactating cows) and individual mammary quarters (lactating cows) from each animal were selected for IHC. Additional tissue sections with RT-qPCR detection and/or histologic lesions were also evaluated by IHC for the detection of NP antigen to confirm a causal link between IAV and the lesion. A Masson's trichrome stain (Newcomer Supply) was performed as per the manufacturer's instructions on representative mammary gland sections from each of the four quarters to highlight fibrous connective tissue. Sections were examined by a veterinary pathologist using an

Olympus BX43 light microscope. Photomicrographs were taken using an Olympus DP28 camera and Olympus cellSens Standard.

Virus detection in clinical samples

IAV RNA extraction and RT–qPCR were performed at the USDA National Veterinary Services Laboratories (NVSL) according to the standard operating procedures as previously described 5,33 . Clinical ante-mortem and necropsy samples were tested using an IAV matrix gene RT–qPCR. A subset of positive samples with Ct \leq 35 was processed for wholegenome sequencing with previously described methods 5 ; and after amplification was completed, we generated cDNA libraries for MiSeq as indicated under virus characterization. A selection of RT–qPCR positive samples with Ct < 30 or milk samples targeted to address impact of immunity on virus isolation were inoculated onto 10-day-old embryonating chicken eggs to determine the presence of viable virus.

Antibody detection

Seroconversion was determined using a blocking ELISA to detect antibodies to the NP (influenza A antibody, IDEXX) according to the manufacturer's instructions for swine at the time of the study with a 1:10 starting dilution of serum or rennet-treated milk and a cutoff sample/negative optical density ratio of 0.6. Before ELISA, milk samples were treated with rennet ($Mucor\ miehei$, Sigma-Aldrich) as previously described ³⁴. H5-specific HI with rooster red blood cells and homologous virus and virus neutralization antibody assays on the London line of MDCK cells with a first passage of MDCK-propagated A/dairy cattle/Texas/24-008749-002/2024 were conducted as previously described ³⁵⁻³⁷. Before HI, sera were heat-inactivated at 56 °C for 30 min, treated with receptor-destroying enzyme (Hardy Diagnostics) and adsorbed with 0.5% and subsequently 100% rooster red blood cells for 20 min each to remove nonspecific haemagglutinin inhibitors and natural serum agglutinins.

Processing of raw sequence data and single nucleotide variant calling

To analyse the Illumina short-read data for 82 samples, we used the Flumina pipeline (https://github.com/flu-crew/Flumina) for processing and analysing influenza data⁴. The pipeline uses Python v3.10, R v4.4 (R Development Core Team 2024), and SnakeMake³⁸ to organize programs and script execution. The reads are preprocessed using FASTP³⁹, removing adaptor contamination, low-complexity sequences and other artefacts. Consensus contigs for phylogenetics were assembled using IRMA v1.1.4 (ref. 26). The pipeline maps cleaned reads to the reference cattle strain derived from sequencing the stock inoculum of A/dairy cattle/Texas/24-008749-002/2024 using BWA (bwa index -a bwtsw)⁴⁰. High-frequency single nucleotide variants (SNVs) were called with GATK v.4.4 (ref. 41), and low-frequency SNVs were called with LoFreq⁴². To assess potential SNV phenotypic changes, a database was generated using the Sequence Feature Variant Types tool from the Influenza Research Database⁴³ for all eight genes. To estimate genome-wide natural selection, we used the program SNPGenie on the VCF files44.

Statistical analysis

Pearson correlation coefficients between Ct values for milk samples from the bucket as well as the inoculated teats (front right and rear left) and rumination time, milk production, and consistency and colour scores of milk from the inoculated teats for all time points were calculating using the package Hmisc v. 5.1-3c in RStudio 2022.02.1+461 'Prairie Trillium'. Correlations were considered significant at P < 0.05 and visualized using the package corrplot v0.92.

Reporting summary

Further information on research design is available in the Nature Portfolio Reporting Summary linked to this article.

Data availability

Data that support the findings of the clinical challenge studies (clinical-challenge-study-data file), sequence data and materials used in the analysis are available via Zenodo at https://zenodo.org/doi/10.5281/zenodo.13126628 (ref. 45). NCBI GenBank accession numbers for sequence data used in the analyses and the raw read sequence data from experimental samples are accessible via Zenodo at https://zenodo.org/doi/10.5281/zenodo.13126628 (ref. 45). Raw sequence data are available in the NCBI Sequence Read Archive, under Bioproject accession number PRINA1102327.

Code availability

Code used in the analysis is available via Zenodo at https://zenodo.org/doi/10.5281/zenodo.13126628 (ref. 45).

- Spackman, E. & Killian, M. L. Avian influenza virus isolation, propagation, and titration in embryonated chicken eggs. Methods Mol. Biol. 2123, 149–164 (2020).
- Shepard, S. S. et al. Viral deep sequencing needs an adaptive approach: IRMA, the iterative refinement meta-assembler. BMC Genomics 17, 708 (2016).
- Katoh, K. & Standley, D. M. MAFFT multiple sequence alignment software version 7: improvements in performance and usability. Mol. Biol. Evol. 30, 772–780 (2013).
- Minh, B. Q. et al. IQ-TREE 2: new models and efficient methods for phylogenetic inference in the genomic era. Mol. Biol. Evol. 37, 1530–1534 (2020).
- Markin, A. et al. Reverse-zoonoses of 2009 H1N1 pandemic influenza A viruses and evolution in United States swine results in viruses with zoonotic potential. *PLoS Pathog.* 19, e1011476 (2023).
- Biosafety in Microbiological and Biomedical Laboratories (Centers for Disease Control and Prevention & National Institutes of Health, 2020); https://www.cdc.gov/labs/pdf/ SF_19_308133-A_BMBL6_00-BOOK-WEB-final-3.pdf
- Waldrep, J. C., Berlinski, A. & Dhand, R. Comparative analysis of methods to measure aerosols generated by a vibrating mesh nebulizer. J. Aerosol Med. 20, 310-319 (2007).
- Cha, M. L. & Costa, L. R. Inhalation therapy in horses. Vet. Clin. North Am. Equine Pract. 33, 29–46 (2017).
- Spackman, E. Avian influenza virus detection and quantitation by real-time RT-PCR. Methods Mol. Biol. 2123, 137–148 (2020).
- Colitti, B. et al. Field application of an indirect gE ELISA on pooled milk samples for the control of IBR in free and marker vaccinated dairy herds. RMC Vet. Res. 14, 387 (2018)
- Killian, M. L. Hemagglutination assay for influenza virus. Methods Mol. Biol. 2123, 3–10 (2020).
- Kitikoon, P., Gauger, P. C. & Vincent, A. L. Hemagglutinin inhibition assay with swine sera. Methods Mol. Biol. 1161, 295–301 (2014).
- Gauger, P. C. & Vincent, A. L. Serum virus neutralization assay for detection and quantitation of serum neutralizing antibodies to influenza A virus in swine. *Methods Mol. Biol.* 2123, 321–333 (2020).
- 38. Molder, F. et al. Sustainable data analysis with Snakemake. F1000Res 10, 33 (2021).
- Chen, S., Zhou, Y., Chen, Y. & Gu, J. fastp: an ultra-fast all-in-one FASTQ preprocessor. Bioinformatics 34, i884-i890 (2018).
- Abente, E. J. et al. A highly pathogenic avian-derived influenza virus H5N1 with 2009 pandemic H1N1 internal genes demonstrates increased replication and transmission in pigs. J. Gen. Virol. 98, 18–30 (2017).
- McKenna, A. et al. The Genome Analysis Toolkit: a MapReduce framework for analyzing next-generation DNA sequencing data. Genome Res. 20, 1297–1303 (2010).
- Wilm, A. et al. LoFreq: a sequence-quality aware, ultra-sensitive variant caller for uncovering cell-population heterogeneity from high-throughput sequencing datasets. Nucleic Acids Res. 40, 11189–11201 (2012).
- Zhang, Y. et al. Influenza Research Database: an integrated bioinformatics resource for influenza virus research. Nucleic Acids Res. 45, D466–D474 (2017).
- Nelson, C. W., Moncla, L. H. & Hughes, A. L. SNPGenie: estimating evolutionary parameters to detect natural selection using pooled next-generation sequencing data. *Bioinformatics* 31, 3709–3711 (2015).
- 45. Anderson, T. flu-crew/dairy-cattle-hpai-experiment: v0.1.1: minor updates to readme and files. Zenodo https://zenodo.org/doi/10.5281/zenodo.13126628 (2024).

Acknowledgements We thank the USDA NADC and NVSL leadership and personnel from animal resource and facilities and engineering units and the NVSL Diagnostic Virology Laboratory, without whom the study could not have been successfully conducted; K. Young, E. Love, S. Anderson, D. Coster, L. Kepler, S. O'Bryon, S. Van Dexter, J. Thompson, J. Fichter and S. Smith for laboratory technical assistance; T. McNunn and the NCAH select agent staff for compliance assistance; R. Cox, J. Huegel, T. Williams, J. Gardner, J. Peterson, E. Hay, E. Pratt and B. Conrad for assistance with animal studies; and P. Plummer, P. Jardon and L. Gimenez-Lirola for discussions on the study and milking equipment. This work was supported in part by the USDA ARS (project number 5030-32000-231-000-D); the National Institute of Allergy and Infectious Diseases, National Institutes of Health, Department of Health and Human Services (contract numbers 75N93021C00015); and the SCINet project and the AI Center of Excellence of the USDA ARS (project numbers 0201-88888-003-000D and 0201-88888-002-000D) Mention of trade names or commercial products in this article is solely for the purpose of providing specific information and does not imply recommendation or endorsement by the US Government. USDA is an equal opportunity provider and employer. Extended Data Fig. 4a,c was created with BioRender.com.

Author contributions A.L.B., B.A., K.S.D., M.V.P., P.B. and A.B. conceived and conducted the study, analysed data and prepared the manuscript. G.C.Z., C.A.S., T.K.A., C.R.H., T.-Q.N., A.M., K.L., E.A.P. and M.K.T. conducted the study, analysed data and prepared the manuscript. S.R.-A., D.R.M. and P.J.G. conceived the study and prepared the manuscript.

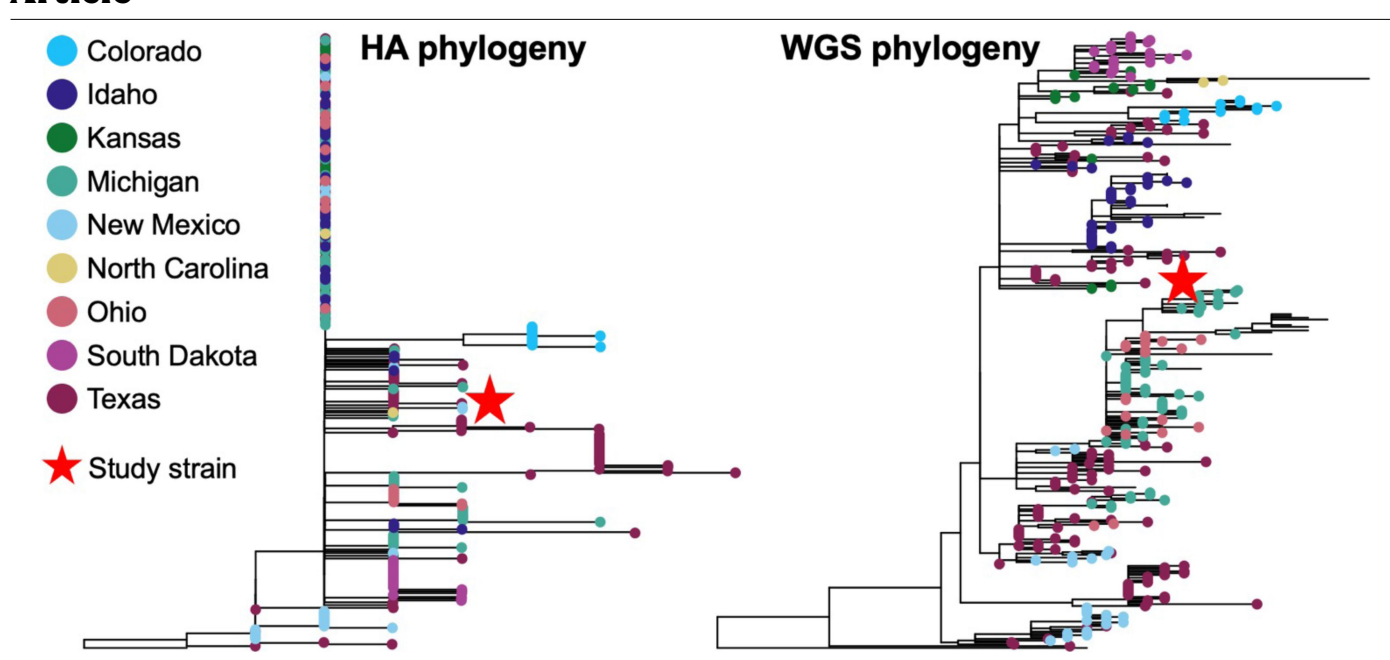
Competing interests The authors declare no competing interests.

Additional information

 $\textbf{Supplementary information} \ The online version contains supplementary material available at \ https://doi.org/10.1038/s41586-024-08166-6.$

Correspondence and requests for materials should be addressed to Amy L. Baker. Peer review information *Nature* thanks Malik Peiris, Lars Larsen and the other, anonymous, reviewer(s) for their contribution to the peer review of this work.

 $\textbf{Reprints and permissions information} \ is \ available \ at \ http://www.nature.com/reprints.$

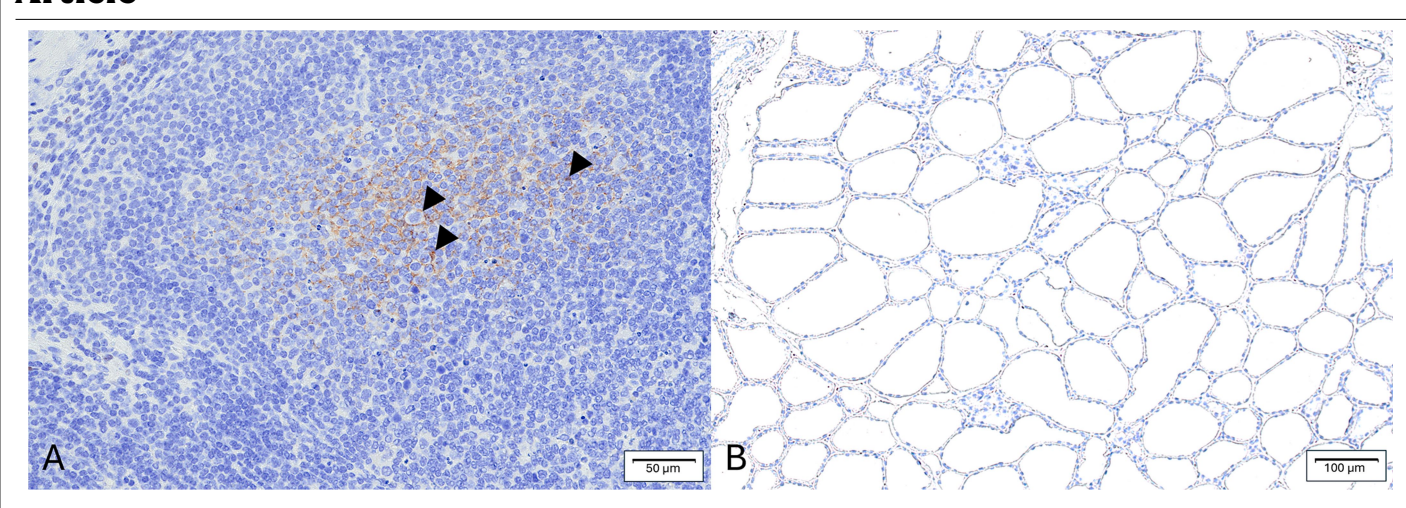


 $\label{lem:extended} \textbf{Extended Data Fig. 1} | \textbf{Evolutionary history of H5N1 clade 2.3.4.4b} \\ \textbf{hemagglutinin genes from dairy cattle in the United States between March} \\ \textbf{and May 2024.} \text{ The HA gene and whole genome phylogeny demonstrated a single introduction of the virus from wild birds to dairy cattle with subsequent dissemination across nine US states. The A/dairy cattle/Texas/24-008749-002/2024 \\ \textbf{Additional Control of the Virus from the A/dairy cattle/Texas/24-008749-002/2024} \\ \textbf{Additional Control of the Virus from the A/dairy cattle/Texas/24-008749-002/2024} \\ \textbf{Additional Control of the Virus from the A/dairy cattle/Texas/24-008749-002/2024} \\ \textbf{Additional Control of the Virus from the A/dairy cattle/Texas/24-008749-002/2024} \\ \textbf{Additional Control of the Virus from the A/dairy cattle/Texas/24-008749-002/2024} \\ \textbf{Additional Control of the Virus from the A/dairy cattle/Texas/24-008749-002/2024} \\ \textbf{Additional Control of the Virus from the A/dairy cattle/Texas/24-008749-002/2024} \\ \textbf{Additional Control of the Virus from the A/dairy cattle/Texas/24-008749-002/2024} \\ \textbf{Additional Control of the Virus from the A/dairy cattle/Texas/24-008749-002/2024} \\ \textbf{Additional Control of the Virus from the A/dairy cattle/Texas/24-008749-002/2024} \\ \textbf{Additional Control of the Virus from the A/dairy cattle/Texas/24-008749-002/2024} \\ \textbf{Additional Control of the Virus from the A/dairy cattle/Texas/24-008749-002/2024} \\ \textbf{Additional Control of the Virus from the A/dairy cattle/Texas/24-008749-002/2024} \\ \textbf{Additional Control of the A/dairy cattle/Texas/24-008749-002/2024} \\ \textbf{Additional Control of C$

study strain, indicated by a red star, was 99.94% identical to a B3.13 whole genome consensus strain (9 nucleotide substitutions across the genome); and at the amino acid level, the TX/24 HA protein was identical to a consensus B3.13 HA sequence, with only 2 synonymous substitutions detected at the nucleotide level.

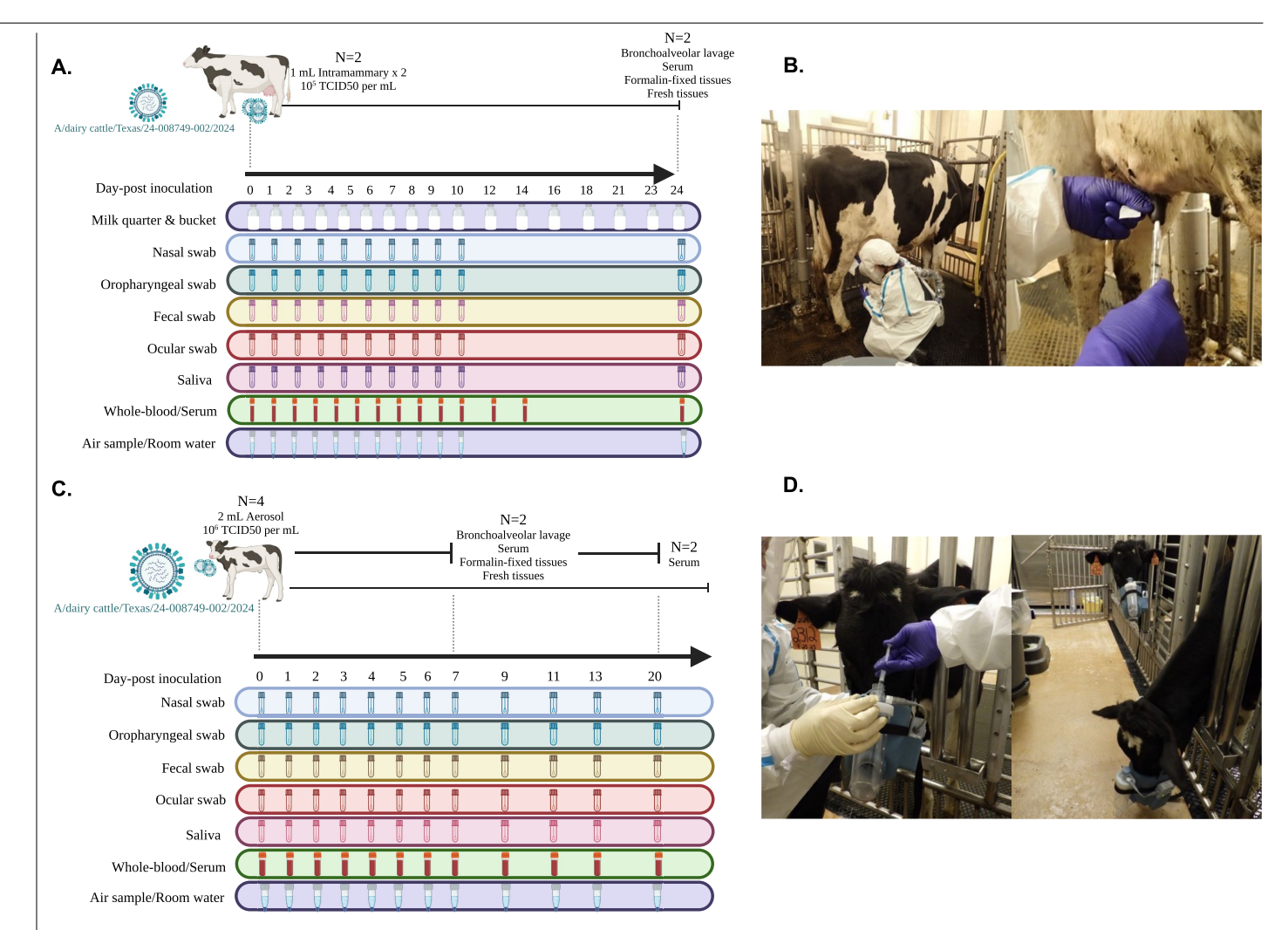


Extended Data Fig. 2 | **Macroscopic lung lesions in a heifer.** Minimal multifocal obstructive atelectasis (arrows and insets) consistent with influenza A virus infection in Heifer 2316.



 $\label{lem:extended} \textbf{Data Fig. 3} | \textbf{Influenza A virus immunohistochemistry in lymph node and mammary gland.} \\ \textbf{Influenza A virus detection by immunohistochemistry (arrowheads) in the germinal center light zone of the supramammary lymph node}$

of cow 2129 (A). Immunohistochemistry did not detect Influenza A virus antigen in the uninoculated left front mammary gland of 2112 (B). Photomicrographs at 200X (A) and 100X (B) magnification.



Extended Data Fig. 4 | Inoculation of Holstein calves and cows. A) Schematic of lactating cow study design. B) Photographs of intramammary inoculation in the lactating Holstein cows via teat canula. C) Schematic of heifer calf study

design. D) Photographs of aerosol respiratory inoculation in the Holstein heifer calves using nebulizer masks. The graphics in \mathbf{a} , \mathbf{c} were created with BioRender.com.

Extended Data Table 1 | Tissues and samples collected at necropsy and tested by RT-qPCR*

	Calf	7 DPI	Calf 2	20 DPI	Cow	24 DPI
Abomasum	out.		out 2		00111	.,,,,,
Blood in MTM						
Brainstem						
Brisket (deep+superficial pectoral)						
Bronchoalveolar lavage fluid						
Cerebellum						
Cerebrum						
Conjunctiva						
Descending colon						
Diaphragm						
Fecal swab						
Feces						
Heart						
Ileum						
Jejunum						
Kidney						
Liver						
LN lleocecal						
LN Inguinal LN Mandibular						
LN Mesenteric						
LN Parotid						
LN Popliteal						
LN Retropharyngeal LN Supramammary						
LN Tracheobronchial						
Lung Accessory lobe						
Lung Caudal left lobe						
Lung Caudal part left cranial lobe						
Lung Caudal part right cranial lobe						
Lung Caudal right lobe Lung Cranial part left cranial lobe						
Lung Cranial part right cranial lobe						
Lung Middle lobe						
-						
Mammary Left front						
Mammary Left rear						
Mammary Right front Mammary Right rear						
Ocular fluid aqueous						
Ocular fluid vitreous						
Omasum						
Pancreas Reticulum						
Rumen						
Rumen content						
Rump (gluteus medius; minimus, biceps femoris)						
Spiral colon						
Spleen						
Tenderloin (psoas major)						
Thymus						
Trachea						
Tracheal swab						
Turbinate						
Urine						

 $^{{}^\}star Each\ column\ represents\ an\ individual\ animal.\ Green=Ct>38, orange=Ct\ 35-38, red=Ct\ <35,\ black=not\ collected.$

$\textbf{Extended Data Table 2} \ | \ \textbf{Positive RT-qPCR samples in aerosol inoculated heifer calves}^*$

DPI	1	2	3	4	5	6	7	CUMULATIVE
Nasal swab	1 (32.3) [#]	1 (24.8)	1 (30.2)	1 (31.6)	1 (27.5)	1 (36.2)	1 (29.8)	7
Oropharyngeal swab (FLOQ)	1 (37.3)	1 (34.9)	2 (34)	1 (36.8)	0	0	0	5
Oropharyngeal swab (COTT)*	1 (37.9)	3 (31.6)	0	1 (36.3)	0	1 (33.4)	0	6
Ocular swab	0	3 (36.8)	0	0	1 (31.4)	0	1 (35.5)	5
Saliva	0	1 (34.2)	2 (35.3)	1 (33.5)	1 (35.3)	1 (37.4)	0	6
CUMULATIVE	3	9	5	4	3	3	2	

 $[\]hbox{\#Number of samples with Ct < 38 out of four and RT-qPCR Ct value or average in parentheses.}$

^{*}Virus isolation was unsuccessful for attempted cotton oropharyngeal swabs. Five FLOQ nasal swabs from 2316 and one FLOQ oropharyngeal swab from 2311 were positive by virus isolation.

Extended Data Table 3 | Raw read data collected from cattle were processed and high- and low-frequency single nucleotide variants (SNVs) were identified

Gene	Coding region change	Functional type	Cattle with variant (#)	Mean allele frequency
MP	T139A	virulence/pathogenicity	1	0.008
MP	S207G	virulence/pathogenicity	1	0.006
NS	T91N, T91A	virulence/pathogenicity	2	0.009
NS	D92E, D92N	virulence/pathogenicity	1	0.009
NS	T94A	virulence/pathogenicity	1	0.009
NS	L95P	virulence/pathogenicity	1	0.012
NS	S99P	virulence/pathogenicity	1	0.007
NS	D101G, D101N	virulence/pathogenicity	2	0.011
NS	F103S	mammal adaptation	1	0.01
NS	D125N	virulence/pathogenicity	1	0.029
PB1	R622Q	virulence/pathogenicity	1	0.028
PB2	L631P	mammal adaptation	1	0.008

Extended Data Table 4 | Antibodies detected in cows and heifers

A. Serum and milk ELISA and hemagglutination inhibition antibody response in lactating dairy cows.*

DPI	0	4	5	6	7	8	9	10	12	14	24	HI 14	HI 24
2112 serum	0.907	1.252	1.265	0.742	0.394	0.296	0.299	0.331	0.338	0.323	0.194	80	80
2129 serum	0.796	1.406	1.533	0.975	0.490	0.353	0.337	0.320	0.335	0.254	0.261	20	160
2112 milk		1.317	1.164	1.000	0.871	0.585	0.481	0.352	0.365	0.270	0.297		#
2129 milk		2.036	1.154	0.939	0.805	0.664	0.473	0.347	0.265	0.255	0.231		#

B. Serum and milk virus neutralizing antibody responses in lactating dairy cows.

ID	Sample	DPI	7	8	9	10	12	14	16	18	21	23	24
2112	Serum		0					640					320
2129	Serum		10					320					640
2112	Front Left		0	0	0	0	20	20	20	10	10	0	10
2112	Front Right		0	0	0	20	160	160	160	80	80	80	40
2112	Rear Left		0	0	0	20	160	320	320	160	160	80	80
2112	Rear Right		0	0	0	0	20	20	10	10	10	0	0
2129	Front Left		0	0	0	20	10	20	20	20	20	0	10
2129	Front Right		0	0	40	80	80	40	80	80	80	40	40
2129	Rear Left		0	10	40	80	80	80	80	80	160	80	40
2129	Rear Right		0	0	0	20	10	20	10	10	20	10	0

C. Serum antibody response in yearling heifers.

	DPI	0	3	7	9	13	20	HI 13	HI 20	VN
2311		0.923	1.252	0.455						
2312		0.783	1.091	0.828	0.974	0.454	0.520	<10	20	20
2313		0.895	1.411	0.900	0.401	0.387	0.370	20	40	40
2316		0.977	1.162	0.499						

$\textbf{A. Serum and milk ELISA} \ and \ he magglutination in hibition antibody \ response \ in \ lactating \ dairy \ cows. \ ^*$

*NP ELISA sample to negative (S/N) ratio of optical densities reported for days post inoculation (DPI) indicated in header row. Hemagglutination inhibition (HI) assay reported as reciprocal titer on 14 and 24 DPI. Positive samples indicated by gray shading and italics; black indicates not tested.

#ELISA S/N reported for pooled milk bucket samples. HI titers in milk at 24 DPI varied by quarter between 10-40 (see data file).

B. Serum and milk virus neutralizing antibody responses in lactating dairy cows.

*Virus neutralization assays reported as reciprocal titers for days post inoculation (DPI) indicated in header row for serum and milk from each mammary quarter. Positive samples indicated by gray shading and italics; black indicates not tested.

C. Serum antibody response in yearling heifers.

*NP ELISA sample to negative (S/N) ratio of optical densities reported for days post inoculation (DPI) indicated in header row. Hemagglutination inhibition (HI) on 13 and 20 DPI and virus neutralization (VN) on 20 DPI reported as reciprocal titer. Positive samples indicated by gray shading and italics; black indicates not tested. Two animals were euthanized on 7 DPI.

Extended Data Table 5 | Clinical scores used to assess dairy calves and lactating dairy cows*

Score	Behavior	Respiratory signs/Rate	Cough	Nasal discharge	Ocular Discharge	Feces
0	Normal	Normal	Normal	Normal, serous discharge	Normal	Normal
1	Mild lethargy with decrease in ambulation and attitude compared to pen mates	Slightly increased respiratory effort/slight dyspnea	Induce single cough	Small amount of unilateral, cloudy discharge	Mild ocular discharge (predominately in canthi)	Semi-formed, pasty
2	Moderate lethargy with stimulation needed to provoke ambulation	Notable increase in respiratory effort/dyspnea	Induce repeated coughs or occasional spontaneous cough	Cloudy or excessive mucus	Moderate bilateral ocular discharge	Loose, but stays on top of bedding or dry and tacky
3	Marked lethargy with ambulation not provoked by stimulation	Severe dyspnea with respiratory distress and tachypnea	Repeated spontaneous coughing	Copious, mucopurulent nasal discharge	Heavy ocular discharge (lashes coated) swelling/erythema of the eyelid	Watery, sifts through bedding

^{*}Adapted from https://www.vetmed.wisc.edu/fapm/svm-dairy-apps/calf-health-scorer-chs/ Calf Health Scorer (CHS) – Food Animal Production Medicine – UW-Madison (wisc.edu).

nature portfolio

Corresponding author(s):	Amy L. Baker
Last updated by author(s):	Sep 13, 2024

Reporting Summary

Nature Portfolio wishes to improve the reproducibility of the work that we publish. This form provides structure for consistency and transparency in reporting. For further information on Nature Portfolio policies, see our <u>Editorial Policies</u> and the <u>Editorial Policy Checklist</u>.

For all statistical analyses, confirm that the following items are present in the figure legend, table legend, main text, or Methods section.

~					
< ⋅	トつ	+1	ıst	11.	\sim
٠,			151	-14	, n

n/a	Confirmed
	\square The exact sample size (n) for each experimental group/condition, given as a discrete number and unit of measurement
\boxtimes	A statement on whether measurements were taken from distinct samples or whether the same sample was measured repeatedly
	The statistical test(s) used AND whether they are one- or two-sided Only common tests should be described solely by name; describe more complex techniques in the Methods section.
	A description of all covariates tested
	A description of any assumptions or corrections, such as tests of normality and adjustment for multiple comparisons
	A full description of the statistical parameters including central tendency (e.g. means) or other basic estimates (e.g. regression coefficient) AND variation (e.g. standard deviation) or associated estimates of uncertainty (e.g. confidence intervals)
	For null hypothesis testing, the test statistic (e.g. <i>F</i> , <i>t</i> , <i>r</i>) with confidence intervals, effect sizes, degrees of freedom and <i>P</i> value noted <i>Give P values as exact values whenever suitable.</i>
\boxtimes	For Bayesian analysis, information on the choice of priors and Markov chain Monte Carlo settings
\boxtimes	For hierarchical and complex designs, identification of the appropriate level for tests and full reporting of outcomes
	Estimates of effect sizes (e.g. Cohen's <i>d</i> , Pearson's <i>r</i>), indicating how they were calculated
	Our web collection on <u>statistics for biologists</u> contains articles on many of the points above.
So	ftware and code
Poli	cy information about <u>availability of computer code</u>
Da	ata collection None

RStudio 2022.02.1+461 "Prairie Trillium", bwa=0.7.17, bioconductor-biostrings=2.66.0, fastp=0.23.4, gatk4=4.5.0.0, lofreg=2.1.5,

python=3.10.14, samtools=1.19, r-doparallel=1.0.17, r-ape=5.7_1, r-data.table=1.14.8, r-essentials=4.2, r-seqinr=4.2_30, r-stringr=1.5.0, r-ape=5.7_1, r-ape=5.7_1,

Data

Data analysis

Policy information about availability of data

All manuscripts must include a <u>data availability statement</u>. This statement should provide the following information, where applicable:

For manuscripts utilizing custom algorithms or software that are central to the research but not yet described in published literature, software must be made available to editors and reviewers. We strongly encourage code deposition in a community repository (e.g. GitHub). See the Nature Portfolio guidelines for submitting code & software for further information.

foreach=1.5.2, snakemake=7.32.4, IRMA v1.1.5, mafft v7.490, IQ-Tree v2.2.2, PARNAS v0.1.5

- Accession codes, unique identifiers, or web links for publicly available datasets
- A description of any restrictions on data availability
- For clinical datasets or third party data, please ensure that the statement adheres to our $\underline{\text{policy}}$

Data that support the findings of the clinical challenge studies and sequence data, code, and materials used in the analysis are available at https://github.com/flucrew/dairy-cattle-hpai-experiment DOI:10.5281/zenodo.13126629.

Research inv	olving hu	man participants, their data, or biological material
Policy information a and sexual orientat		vith human participants or human data. See also policy information about sex, gender (identity/presentation), thnicity and racism.
Reporting on sex	and gender	N/A
Reporting on race other socially rele groupings		N/A
Population chara	cteristics	N/A
Recruitment		N/A
Ethics oversight		N/A
Note that full informa	ation on the appro	oval of the study protocol must also be provided in the manuscript.
Field-spe	ecific re	porting
•		s the best fit for your research. If you are not sure, read the appropriate sections before making your selection.
Life sciences		
		ehavioural & social sciences
Tot a reference copy of t	the document with	in sections, see <u>nature conjugate in reporting summary nacipal</u>
Life scier	nces stu	ıdy design
All studies must dis	close on these	points even when the disclosure is negative.
Sample size		rs and 2 lactating Holstein dairy cows. No sample size calculation was performed. The groups sizes were determined by space in the BSL3-Ag high containment facility.
Data exclusions	None.	
Replication	Due to the restr	riction of BSL3-Ag containment, the study sample size is limited and there were no replicates.
Randomization	Animals were ra	andomly chosen based upon availability.
Blinding	Blinding was no	t possible but not necessary as tests were not subjective.
Reportin	g for sr	pecific materials, systems and methods
•	<u> </u>	about some types of materials, experimental systems and methods used in many studies. Here, indicate whether each material,
system or method list	ted is relevant to	your study. If you are not sure if a list item applies to your research, read the appropriate section before selecting a response.
Materials & exp	perimental s	ystems Methods
n/a Involved in th	ne study	n/a Involved in the study
Antibodies		ChIP-seq
Eukaryotic	cell lines	Flow cytometry
Palaeontol	ogy and archaeol	ogy MRI-based neuroimaging
Animals an	d other organism	
Clinical dat	a	
Dual use re	esearch of concer	n
Plants		

Antibodies used

rabbit polyclonal anti-influenza A NP (GeneTex, https://www.genetex.com) used for IHC at 1:2000 dilution

Validation

https://www.genetex.com/MarketingMaterial/Index/five_pillars

CCII	IIIIC.
	cell

Policy information about <u>cell lines</u>	and sex and Gender in Research
Cell line source(s)	Madin-Darby Canine Kidney cells, London Line (Cat # FR-58, International Reagent Resource)
Authentication	Cells were not authenticated
Mycoplasma contamination	Cells were not tested for mycoplasma
Commonly misidentified lines (See ICLAC register)	None

Animals and other research organisms

Policy information about <u>studies involving animals</u>; <u>ARRIVE guidelines</u> recommended for reporting animal research, and <u>Sex and Gender in Research</u>

Laboratory animals	Holstein cattle of 1 year of age (n=5) and 3 years of age (n=2)
Wild animals	None
Reporting on sex	All female due to nature of disease
Field-collected samples	None
Ethics oversight	Approved by the institutional animal care and use committee of the USDA ARS National Animal Disease Center

Note that full information on the approval of the study protocol must also be provided in the manuscript.

Plants

Seed stocks	N/A
Novel plant genotypes	N/A
Authentication	N/A